J|A|C|S
ARTICLES
Published on Web 11/04/2006

Supramolecular Bis(rutheniumphthalocyanine)−Perylenediimide Ensembles: Simple Complexation as a Powerful Tool toward Long-Lived Radical Ion Pair States

M. Salomé Rodríguez-Morgade,[†] Tomás Torres,*[,†]
Carmen Atienza-Castellanos,[‡] and Dirk M. Guldi*[,‡]

Contribution from the Departamento de Química Orgánica (C-I), Universidad Autónoma de Madrid, Cantoblanco, E−28049 Madrid, Spain, and Friedrich-Alexander-Universität Erlangen-Nürnberg, Institute for Physical Chemistry, Egerlandstr. 3, D-91058 Erlangen, Germany

Received March 31, 2006; E-mail: tomas.torres@uam.es; dirk.guldi@chemie.uni-erlangen.de

Abstract: A novel supramolecular electron donor−acceptor hybrid (**1**) has been designed through axial coordination of a perylenebisimide moiety [BPyPDI], bearing two 4-pyridyl substituents at the imido positions, to the ruthenium(II) metal centers of two phthalocyanines [Ru(CO)Pc]. This modular protocol enables access to electron donor−acceptor hybrids with potentially great design flexibility. The new array (**1**) has been characterized by standard spectroscopic methods, and its photophysical behavior has been established by using ultrafast and fast time-resolved techniques. Photoexcitation of either chromophore leads to a product that is essentially identical for both pathways, that is, evolving from the [Ru(CO)Pc] or [BPyPDI] singlet excited state. Features of the photoproduct are new transient maxima at 530 and 725 nm, plus transient minima at 580 nm and 650 nm. Based on the radiolytically generated [BPyPDI$^{\bullet-}$] (i.e., one-electron reduction of [BPyPDI]) and [Ru(CO)Pc$^{\bullet+}$] (i.e., one-electron oxidation of [Ru(CO)Pc]) features, which in the 300 and 900 nm range remarkably resemble those noted for photoexcited **1**, we attribute the photolytically generated species to the composite spectrum of the [Ru(CO)Pc$^{\bullet+}$−BPyPDI$^{\bullet-}$−RuCOPc] radical ion pair state. Its lifetime, which is on the order of 115 ± 5 ns, reveals a significant stabilization and confirms that the strongly exothermic charge recombination dynamics are placed deeply in the inverted region of the Marcus parabola.

Introduction

Developing renewable energy and energy efficiency technologies along with advancing the science behind them is emerging as one of the most imperative challenges that our society faces. A fascinating strategy, and perhaps the most realistic one in the long run, consists of mimicking nature, that is, harvesting and converting sunlight, as a means to provide clean, reliable, affordable solar electricity.[1] The in-depth study of energy-related materials and devices envisages the storage of energy that is associated with (i) the initial radiation in the form of highly energetic/reactive chemicals and (ii) the *on-demand* production of energy equivalents. Some preeminent examples comprise a popular power source for some consumer electronic devices, including calculators, watches, radios, lanterns and other small battery charging applications.

With this ultimate goal in mind, a great assortment of sophisticated and versatile systems has been constructed, leading to tremendous advances in the areas of solar photochemistry and solar energy conversion.[2] Implicit is that the design of chemical architectures, which function as complex but still highly efficient photosynthetic systems, is by no means a trivial task.[3] A successful and widely applied strategy is to dissect the photosynthetic apparatus into functional subunits (i.e., photosynthetic reaction center and light harvesting antennae) that perform separate half cell reactions. In a complementary step, these modular entities are brought together and integrated into a single device. Although this modular approach still implies a high degree of complexity, it provides a better understanding of the complicated and multifaceted mechanism of photosynthesis and assists in the rational design of a novel, and maybe even better performing, photosynthetic apparatus.

Multifunctionality, as a leading paradigm in designing electron donors and electron acceptors, has become an indispensable target in the fields of solar photochemistry and solar

[†] Universidad Autónoma de Madrid.
[‡] Friedrich-Alexander-Universität Erlangen-Nürnberg.

(1) Eisenberg, R.; Nocera, D. G. *Inorg. Chem.* **2005**, *44*, 6799−6801.
(2) (a) Wasielewski, M. R. *Chem. Rev.* **1992**, *92*, 435−461. (b) Gust, D.; Moore, T. A.; Moore, A. L. *Acc. Chem. Res.* **2001**, *34*, 40−48. (c) Arakawa, H. et al. *Chem. Rev.* **2001**, *101*, 953−996. (d) Alstrum-Acevedo, J. H.; Brennaman, M. K.; Meyer, T. J. *Inorg. Chem.* **2005**, *44*, 6802−6827. (e) Chakraborty, S.; Wadas, T. J.; Hester, H.; Schmehl, R.; Eisenberg, R. *Inorg. Chem.* **2005**, *44*, 6865−6878.
(3) (a) *The Photosynthetic Reaction Center*; Deisenhofer, J., Norris, J. R., Eds.; Academic Press: New York, 1993. (b) *Molecular Mechanisms of Photosynthesis*; Blankenship, R. E., Ed.; Blackwell Science, 2002.

energy conversion. Such systems mimic the basics of one of the key steps in photosynthesis, namely, photoinduced charge separation.[4,5] Donor−acceptor ensembles also play key roles in molecular photovoltaic[6] and photogalvanic[7] devices, whose ultimate function is the direct conversion of the energy stored in the photogenerated radical ion pair states into electrical power. Hereby, a basic requirement is that the donor's excited state must be sufficiently reducing to mediate the transfer of electrons to the acceptor units. A great deal of work in this field is based on *nature-inspired* porphyrin−quinone arrays.[2a,b,8] Nevertheless, the introduction of other electroactive units and/or chromophores has also been probed.[2e,9]

Phthalocyanines (Pc)[10] have emerged as a promising molecular component for artificial photosynthetic apparatus, since they (i) exhibit large absorption cross sections in the visible region, (ii) contain large, conjugated π-systems suitable for efficient electron-transfer processes, and (iii) possess strongly reducing or oxidizing characteristics determined by the nature of the peripheral functions.[11]

Our keen interest in Pc building blocks has led us to synthesize a wide range of Pc-containing electron donor−acceptor conjugates and/or hybrids, in which the complementary electroactive units are of diverse nature and/or redox character.[12] In this context, we have designed and studied several series of either covalently linked phthalocyanine−fullerene conjugates[11d,e,h,13] or supramolecularly assembled phthalocyanine−fullerene hybrids.[11f,g,14,15] Some of the aforementioned hybrid structures also exhibited promising performances as constituents of photovoltaic devices.[13c,16]

The objective of the current work was to prepare a novel electron donor−acceptor hybrid, in which a perylenediimide chromophore constitutes the acceptor unit. The chemical structure of perylenediimide is very appealing − at least from a purely synthetic point of view − since this molecule can be easily forged for a modular building block synthesis.[17] From a functional standpoint, perylene dyes have been used extensively as light absorbers, energy-transfer agents, and charge carriers.[18,19] However, among the very few reported Pc−perylenediimide ensembles,[11i,20,21] to date only one of them, namely, a covalently linked phthalocyanine−perylenediimide array, has

(4) (a) Balzani, V. *Supramolecular Photochemistry*; D. Reidel Publishing Co.: Dordrecht, Holland, 1987. (b) Balzani, V.; Moggi, L.; Scandola, F. Towards a Supramolecular Photochemistry: Assembly of Molecular Components to Obtain Photochemical Molecular Devices. In *Supramolecular Photochemistry*; Balzani, V., Ed.; D. Reidel Publishing Co.: Dordrecht, Holland, 1987; pp 1−28.

(5) (a) *Electron Transfer in Chemistry*; Balzani, V., Ed.; Wiley-VCH: Weinheim, Germany, 2001. (b) Turro, N. J. *Modern Molecular Photochemistry*; University Science Books: Mill Valley, CA, 1991; pp 321−361. (c) Speiser, S. *Chem. Rev.* **1996**, *96*, 1953−1976.

(6) (a) O'Regan, B.; Grätzel, M. *Nature (London)* **1991**, *353*, 737. (b) Grätzel, M. *Inorg. Chem.* **2005**, *44*, 6841−6851. (c) Meyer, G. J. *Inorg. Chem.* **2005**, *44*, 6852−6854.

(7) Albery, W. J. *Acc. Chem. Res.* **1982**, *15*, 142.

(8) (a) Gust, D.; Moore, T. A.; Moore, A. L. *Acc. Chem. Res.* **1993**, *26*, 198−205. (b) Kurreck, H.; Huber, M. *Angew. Chem.* **1995**, *107*, 929−947. *Angew. Chem., Int. Ed. Engl.* **1995**, *34*, 849−866. (c) Huber, M. *Eur. J. Org. Chem.* **2001**, *23*, 4379−4389.

(9) (a) Imahori, H.; Yamada, H.; Guldi, D. M.; Endo, Y.; Shimomura, A.; Kundu, S.; Yamada, K.; Okada, T.; Sakata, Y.; Fukuzumi, S. *Angew. Chem., Int. Ed.* **2002**, *41*, 2344−2347. (b) Balzani, V.; Credi, A.; Venturi, M. *Photoinduced Charge Separation and Solar Energy Conversion in Molecular Devices and Machines: A Journey into the Nanoworld*; Balzani, V., Credi, A., Venturi M., Eds.; Wiley-VCH: Weinheim, Germany, 2003; pp 132−173. (c) Sanchez, L.; Sierra, M.; Martin, N.; Myles, A. J.; Dale, T. J.; Rebek, J., Jr.; Seitz, W.; Guldi, D. M. *Angew. Chem., Int. Ed.* **2006**, *45*, 4637−4641. (d) Martin, N. *Chem. Commun.* **2006**, 2093−2104.

(10) (a) *Phthalocyanines: Properties and Applications*; Leznoff, C. C., Lever, A. B. P., Eds.; VCH: Weinheim, Germany, 1989, 1993, 1996; Vols. 1−4. (b) Hanack, M.; Heckmann, H.; Polley, R. In *Methods in Organic Chemistry (Houben-Weyl)*; Schaumann, E., Ed.; Thieme: Stuttgart, 1998; Vol. E 9d, p 717. (c) de la Torre, G.; Nicolau, M.; Torres, T. In *Phthalocyanines: Synthesis, Supramolecular Organization and Physical Properties (Supramolecular Photosensitive and Electroactive Materials)*; Nalwa, H. S., Ed.; Academic Press: New York, 2001. (d) Rodríguez-Morgade, M. S.; de la Torre, G.; Torres, T. In *The Porphyrin Handbook*; Kadish, K. M., Smith, K. M., Guilard, R., Eds.; Academic Press: San Diego, CA, 2003; Vol. 13. (e) *The Porphyrin Handbook*; Kadish, K. M., Smith, K. M., Guilard, R., Eds.; Academic Press: San Diego, CA, 2003; Vols. 15−20. (f) Duro, J. A.; Torres, T. *Chem. Ber.* **1993**, *126*, 269−271. (g) de la Torre, G.; Vázquez, P.; Agulló-López, F.; Torres, T. *J. Mater. Chem.* **1998**, *8*, 1671−1683. (h) de la Torre, G.; Vázquez, P.; Agulló-López, F.; Torres, T. *Chem. Rev.* **2004**, *104*, 3723−3750.

(11) (a) Maya, E. M.; García-Frutos, E. M.; Vázquez, P.; Torres, T.; Martín, G.; Rojo, G.; Agulló-Lopez, F.; González-Jonte, R. H.; Ferro, V. R.; García de la Vega, J. M.; Ledoux, I.; Zyss, J. *J. Phys. Chem. A* **2003**, *107*, 2110−2117. (b) Maya, E. M.; García, C.; García-Frutos, E. M.; Vázquez, P.; Torres, T. *J. Org. Chem.* **2000**, *65*, 2733−2739. (c) Maya, E. M.; Vázquez, P.; Torres, T. *Chem.−Eur. J.* **1999**, *5*, 2004−2013. (d) Gouloumis, A.; Liu, S. G.; Sastre, A.; Vázquez, P.; Echegoyen, L.; Torres, T. *Chem.−Eur. J.* **2000**, *6*, 3600−3607. (e) Guldi, D. M.; Gouloumis, A.; Vázquez, P.; Torres, T. *Chem. Commun.* **2002**, 2056−2057. (f) Guldi, D. M.; Ramey, J.; Martínez-Díaz, M. V.; de la Escosura, A.; Torres, T.; Da Ros, T.; Prato, M. *Chem. Commun.* **2002**, 2774−2775. (g) Martínez-Díaz, M. V.; Fender, N. S.; Rodríguez-Morgade, M. S.; Gómez-López, M.; Diederich, F.; Echegoyen, L.; Stoddart, J. F.; Torres T. *J. Mater. Chem.* **2002**, *12*, 2095−2099. (h) Guldi, D. M.; Zilbermann, I.; Gouloumis, A.; Vázquez, P.; Torres, T. *J. Phys. Chem. B* **2004**, *108*, 18485−18494. (i) Li, X.; Sinks, L. E.; Rybtchinski, B.; Wasielewski, M. R. *J. Am. Chem. Soc.* **2004**, *126*, 10810−10811.

(12) (a) González-Cabello, A.; Vázquez, P.; Torres, T. *Tetrahedron Lett.* **1999**, *40*, 3263−3266. (b) Gouloumis, A.; Liu, S.-G.; Vázquez, P.; Echegoyen, L.; Torres, T. *Chem. Commun.* **2001**, 399−400. (c) González-Cabello, A.; Vázquez, P.; Torres, T.; Guldi, D. M. *J. Org. Chem.* **2003**, *68*, 8635−8642. (d) González-Rodríguez, D.; Claessens, C. G.; Torres, T.; Liu, S.; Echegoyen, L.; Vila, N.; Nonell, S. *Chem.−Eur. J.* **2005**, *11*, 3881−3893.

(13) (a) Sastre, A.; Gouloumis, A.; Vázquez, P.; Torres, T.; Doan, V.; Schwartz, B. J.; Wudl, F.; Echegoyen, L.; Rivera, J. *Org. Lett.* **1999**, *1*, 1807−1810. (b) González-Rodríguez, D.; Torres, T. In *The Exciting World of Nanocages and Nanotubes*; Kamat, P., Guldi, D. M., Kadish, K., Eds.; ECS: Pennington, NJ, 2002; Vol. 12, pp 195−210. (c) Loi, M. A.; Neugebauer, H.; Denk, P.; Brabec, C. J.; Sariciftci, N. S.; Gouloumis, A.; Vázquez, P.; Torres, T. *J. Mater. Chem.* **2003**, *13*, 700−704. (d) Guldi, D. M.; Gouloumis, A.; Vázquez, P.; Torres, T.; Georgakilas, V.; Prato, M. *J. Am. Chem. Soc.* **2005**, *127*, 5811−5813.

(14) (a) Doyle, J. J.; Ballesteros, B.; de la Torre, G.; Torres, T.; Blau, W. J.; *Chem. Phys. Lett.* **2006**, *428*, 307−311. (b) Ballesteros, B.; de la Torre, G.; Torres, T.; Hug, G. L.; Rahmanc, G. M. A.; Guldi, D. M. *Tetrahedron* **2006**, *62*, 2097−2101.

(15) For some examples of Pc-C_{60} assemblies reported by other research groups, see: (a) Linssen, T. G.; Durr, K.; Hanack, M.; Hirsch, A. *J. Chem. Soc., Chem. Commun.* **1995**, 103−104. (b) Durr, K.; Fiedler, S.; Linssen, T.; Hirsch, A.; Hanack, M. *Chem. Ber.* **1997**, *130*, 1375−1378. (c) Tian, Z.; He, C.; Liu, C.; Yang, W.; Yao, J.; Nie, Y.; Gong, Q.; Liu, Y. *Mater. Chem. Phys.* **2005**, *94*, 444−448. (d) Kim, K. N.; Choi, C. S.; Kay, K.-Y. *Tetrahedron Lett.* **2005**, *46*, 6791−6795. (d) Chen, Y.; El-Khouly, M. E.; Sasaki, M.; Araki, Y.; Ito, O. *Org. Lett.* **2005**, *7*, 1613−1616. (e) Kim, D. J.; Kay, K.-Y.; Kang, E. S. *Abstracts of Papers, 226th ACS National Meeting*; New York, United States, September 7−11, 2003, ORGN-424.

(16) (a) Loi, M. A.; Denk, P.; Hoppe, H.; Neugebauer, H.; Meissner, D.; Winder, C.; Brabec, C. J.; Sariciftci, N. S.; Gouloumis, A.; Vazquez, P.; Torres, T. *Synth. Met.* **2003**, *137*, 1491−1492. (b) Neugebauer, H.; Loi, M. A.; Winder, C.; Sariciftci, N. S.; Cerullo, G.; Gouloumis, A.; Vázquez, P.; Torres, T. *Sol. Energy Mater. Sol. Cells* **2004**, *83*, 201−209.

(17) Perylenediimides possess two distinct chemical zones, namely the bay region and imido position, that can be easily functionalized independently one from the other. Thus, this kind of dye is ideally suited for the modular construction of geometrically diverse molecular and supramolecular architectures. For example, see: ref 19c and also (a) Würthner, F.; Sautter, A.; Schmid, D.; Weber, P. J. A. *Chem.−Eur. J.* **2001**, *7*, 894−902. (b) Kohl, C.; Weil, T.; Du, J.; Müllen, K. *Chem.−Eur. J.* **2004**, *10*, 5297−5310. (c) Ahrens, M. J.; Sinks, L. E.; Rybtchinski, B.; Liu, W.; Jones, B. A.; Giaimo, J. M.; Gusev, A. V.; Goshe, A. J.; Tiede, D. M.; Wasielewski, M. R. *J. Am. Chem. Soc.* **2004**, *126*, 8284−8294. (d) Ego, C.; Marsitzky, D.; Becker, S.; Zhang, J.; Grimsdale, A. C.; Müllen, K.; MacKenzie, J. D.; Silva, C.; Friend, R. H. *J. Am. Chem. Soc.* **2003**, *125*, 437−443.

(18) Würthner, F. *Chem. Commun.* **2004**, 1564−1579.

(19) For some examples, see: (a) Zollinger, H. *Color Chemistry: Syntheses, Properties and Applications of Organic Dyes and Pigments*; VCH: Weinheim, 1991. (b) Yang, S. I.; Lammi, R. K.; Prathapan, S.; Miller, M. A.; Seth, J.; Diers, J. R.; Bocian, D. F.; Lindsey, J. S.; Holten, D. *J. Mater. Chem.* **2001**, *11*, 2420−243. (c) Rybtchinski, B.; Sinks, L. E.; Wasielewski, M. R. *J. Am. Chem. Soc.* **2004**, *126*, 12268−12269. (d) van der Boom, T.; Hayes, R. T.; Zhao, Y.; Bushard, P. J.; Weiss, E. A.; Wasielewski, M. R. *J. Am. Chem. Soc.* **2002**, *124*, 9582−9590.

(20) (a) Signerski, R.; Jarosz, G.; Godlewski, J. *Synth. Met.* **1998**, 135−137. (b) Liu, S.-G.; Liu, Y.-Q.; Xu, Y.; Jiang, X.-Z.; Zhu, D.-B. *Tetrahedron Lett.* **1998**, *39*, 4271−4274. (c) Fukuzumi, S.; Ohkubo, K.; Ortiz, J.; Gutiérrez, A. M.; Fernández-Lázaro, F.; Sastre-Santos, A. *Chem. Commun.* **2005**, *30*, 3814−3816.

(21) Lindsey and co-workers have reported a phthalocyanine−porphyrin−perylenemonoimide triad. See: Miller, M. A.; Lammi, R. K.; Prathapan, S.; Holten, D.; Lindsey, J. S. *J. Org. Chem.* **2000**, *65*, 6634−6649.

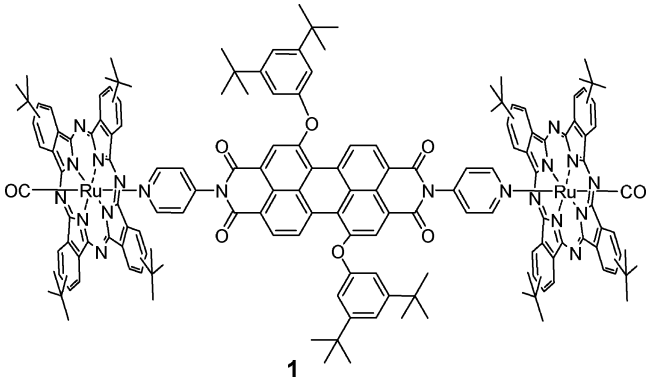

1

Figure 1. [Ru(CO)Pc−BPyPDI−Ru(CO)Pc] **1**.

been shown to afford a long-lived radical ion pair state.[20c,22] Herein, we wish to report a novel, supramolecular bis(phthalocyanine)−perylenediimide donor−acceptor hybrid (**1**) (Figure 1), composed of a perylene-(bis)imide dye [BPyPDI] linked to two ruthenium(II) phthalocyanines [Ru(CO)Pc] via strong metal coordination.[23] The photophysical properties of this construct are examined in detail.

Results and Discussion

Synthesis and Characterization of Molecular Precursors. Despite their unlike chemical structures, Pc and perylenediimide chromophores bear a number of similar characteristics. For example, both dyes are aromatic, planar compounds that display a strong tendency to aggregate in solution. In addition, both unsubstituted phthalocyanine and perylenediimide are very insoluble in organic solvents. Therefore, functionalization of both molecular precursors evolves as a necessity. Hereby, the choice of the substituent is decisive for issues such as handling, reactivity, and characterization.

In the context of Pc's, tetra-*tert*-butylphthalocyanines were selected, since four *tert*-butyl substituents are expected to ensure high solubility, reduce aggregation in solution, and provide σ-donor features. As a consequence, the corresponding Pc will bear strong electron donor character.[11c,d,12a−c,13,14a] Likewise, functionalization at the bay region of the perylenediimide moiety with di-*tert*-butylphenoxy groups guarantees solubility and avoids aggregation,[17c] without, however, compromising the electron-acceptor character of the dye.

The synthesis of the [Ru(CO)Pc] **2** (see structure in Scheme 1) was carried out by metalation of the tetra-*tert*-butylphthalocyanine free base using $Ru_3(CO)_{12}$ in refluxing phenol. The reaction was monitored by UV/vis spectroscopy to the point

Scheme 1. Synthesis of [Ru(CO)Pc−BPyPDI−Ru(CO)Pc] **1**

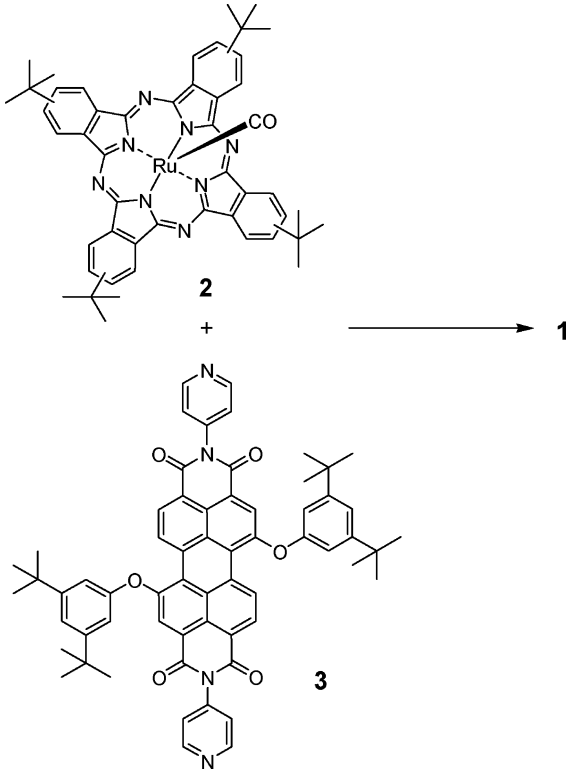

that no more free base was detected. The metalation yielded, after purification by chromatography, 82% of [Ru(CO)Pc] **2** as a mixture of regioisomers. The most characteristic spectroscopic feature of **2** is an IR band at 1958 cm^{-1}, together with a less intense band at 2042 cm^{-1}, that corresponds to the ν(C═O) stretching modes; see Supporting Information.[24] The ^{1}H NMR spectrum in deuterated chloroform revealed the aromatic protons as four broad signals between 9.7 and 7.8 ppm and two additional ones at 5.8−5.5 ppm. In contrast, when the spectrum was measured in DMSO-d_6, the aromatic region was much simpler and displayed only two broad signals at 9.4−8.8 and 8.3−8.1 ppm. A similar spectrum was obtained upon addition of a drop of deuterium oxide to the chloroform solution of **2**. These results can be rationalized by considering a partial *face-to-face* aggregation of [Ru(CO)Pc] **2** when dissolved in chloroform. The nonaggregated, monomeric species relates to signals at 9.7−9.3 and 8.5−8.1 ppm, corresponding to the protons at the *ortho* and *meta* positions, respectively, of the phthalocyanine fused benzene rings. Coordinating solvents, such as dimethyl sulfoxide and water, prevent aggregation of **2** and shift the equilibrium toward monomeric macrocycles through their axial coordination with the ruthenium(II) ion.[24a] It is likely that **2** also coordinates water in the solid state, as the IR spectrum suggests.

The UV/vis spectrum of **2** displays Soret- and Q-band absorptions at 296 and 652 nm, respectively. Such maxima imply a notable blue shift relative to other tetra-*tert*-butyl-substituted metallophthalocyanines.[25] This is in agreement with

(22) Some porphyrin−perylenediimide arrays have been reported and studied for photoinduced electron-transfer processes. For some recent examples, see: ref 19d and also (a) Prodi, A.; Chiorboli, C.; Scandola, F.; Lengo, E.; Alessio, E.; Dobrawa, R.; Würthner, F. *J. Am. Chem. Soc.* **2005**, *127*, 1454−1562. (b) Xiao, S.; El-Khouly, M. E.; Li, Y.; Gan, Z.; Liu, H.; Jiang, L.; Araki, Y.; Ito, O.; Zhu, D. *J. Phys. Chem. B* **2005**, *109*, 3658−3667. (c) Liu, Y.; Wang, N.; Li, Y.; Liu, H.; Li, Y.; Xiao, J.; Xu, X.; Huang, C.; Cui, S.; Zhu, D. *Macromolecules* **2005**, *38*, 4880−4887. (d) You, C.-C.; Würthner, F. *Org. Lett.* **2004**, *6*, 2401−2404. (e) Liu, M. O.; Tai, C.-H.; Chen, C.-W.; Chang, W.-C.; Hu, An. T. *J. Photochem. Photobiol., A* **2004**, *163*, 259−266. (f). Loewe, R. S.; Tomizaki, K.-Y.; Chevalier, F.; Lindsey, J. S. *J. Porphyrins Phthalocyanines* **2002**, *6*, 626−642. (g) Yang, S. I.; Prathapan, S.; Miller, M. A.; Seth, J.; Bocian, D. F.; Lindsey, J. S.; Holten, D. *J. Phys. Chem. B* **2001**, *105*, 8249−8258.

(23) Despite the strength of Ru−pyridyl coordination bonds, in this kind of array the pyridyl substituents, and hence the phthalocyanine moieties, are electronically decoupled from the perylenediimide counterpart, due to the presence of nodes at the imido nitrogens in the HOMO and LUMO of this red chromophore. See: refs 18, 22a and also Mercadante, R.; Trsic, M.; Duff, J.; Aroca, R. *THEOCHEM* **1997**, *394*, 215−226.

(24) (a) Enakieva, Y. Y.; Gorbunova, Y. G.; Sakharov, S. G.; Tsivadze A. Y. *Russ. J. Inorg. Chem.* **2002**, *47*, 1815−1820. (b) Gorbunova, Y. G.; Enakieva, Y. Y.; Sakharov, S. G.; Tsivadze, A. Y. *Russ. Chem. Bull. Int. Ed.* **2004**, *53*, 74−79.

(25) For example, tetra-*tert*-butylphthalocyanine bearing Zn(II) within its central binding core shows B- and Q-bands at λ_{max} = 348 and 678 nm, respectively.

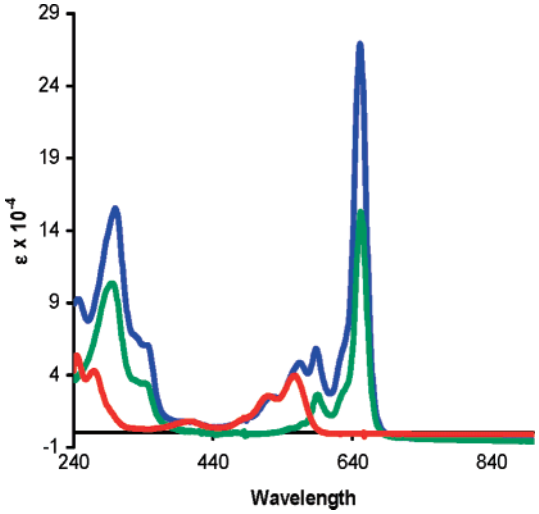

Figure 2. UV/vis spectra of [Ru(CO)Pc] **2** (green line), [BPyPDI] **3** (red line), and supramolecular [Ru(CO)Pc-BPyPDI−Ru(CO)Pc] **1** (blue line) in chloroform.

previous reports on RuPc's[24,26] and has been attributed to substantially enhanced metal−Pc interactions.[26e] Finally, the structure of **2** was confirmed by MS spectrometry (MALDI-TOF) through peaks at m/z= 860−870 and m/z= 832−841. The former peak corresponds to the molecular cluster of $[M]^+$, while we assign the latter to $[M-CO]^+$.

Perylene derivative **3** bearing two 4-pyridyl substituents at the imido positions was obtained in good yield by treating the corresponding 1,7-bis(3′,5′-di-*tert*-butylphenoxy)perylene-3,4:9,10-tetracarboxydianhydride[17c] with 4-aminopyridine in the presence of $Zn(OAc)_2$.[17a] The red pigment was characterized by ^{1}H NMR (see Figure 3), ^{13}C NMR, IR, and UV/vis (Figure 2) spectroscopy and MS spectrometry.

Synthesis and Characterization of [Ru(CO)Pc−BPyPDI−Ru(CO)Pc] 1. Control over the geometry of **1** is realized through the utilization of phthalocyanine derivatives that host Ru centers within their central cavity. Such metallomacrocycles form stable and rigid architectures through metal coordination of, for example, pyridine derivatives.[27] Importantly, single ligation at the Ru(II) center of the phthalocyanine is assured by placing a strongly ligating, π-acceptor carbonyl ligand at one of the two axial Ru(II) coordination sites. This directs the perylenediimide-bispyridyl ligand [BPyPDI] to the opposite axial coordination site.[22a,26a,b]

Therefore, **1** was assembled in 68% yield by treating 2 equiv of [Ru(CO)Pc] **2** with 1 equiv of [BPyPDI] **3** in chloroform at room temperature (Scheme 1).

The structure of **1** was established on the basis of its spectroscopic features, namely, MS, IR, ^{1}H NMR, ^{13}C NMR, and UV/vis. The MS spectrum (MALDI-TOF), for example, displays a cluster at m/z = 2679−2692, which corresponds to the theoretically determined pattern for $[M]^+$; see Supporting Information. The most remarkable IR spectroscopy attribute of **1** is a band at 1969 cm^{-1}, due to the presence of the carbonyl ligands coordinated to the Ru(II) ion, and two bands at 1713 and 1678 cm^{-1}, which correspond to the imido carbonyl functionality.

Compound **1** is reasonably stable at concentrated solutions in noncoordinating solvents and when protected from extensive light exposure. No changes were, for example, observed by ^{1}H NMR after 24 h in a 7.45 M solution of chloroform. Likewise, UV/vis spectrophotometry indicates no variation in a concentration range between 3.35 × 10^{-6} M and 4.09 × 10^{-5} M. The scarce solubility of complex **1** in coordinating solvents (i.e., acetonitrile) prevented a meaningful stability analysis. The absorption spectrum of **1** is presented in Figure 2, together with the corresponding spectra of the molecular units (i.e., **2** and **3**).

The UV/vis spectra do not imply any electronic coupling between the [Ru(CO)Pc] and [BPyPDI] subunits in the ground state.[23] In fact, the electronic spectrum of **1** is best described as the sum of its molecular components in a 2:1 ratio. Moreover, no absorption that might be attributable to a charge transfer is seen in the recorded range of up to 900 nm; see Figure 2.

Figure 3 represents a comparison between the ^{1}H NMR spectra of **1** and **3** and provides unequivocal grounds for the formation of **1** and its characterization. In **1**, [BPyPDI] is located between the two [Ru(CO)Pc] rings in such a geometric orientation that it experiences the influence of the diamagnetic ring currents of [Ru(CO)Pc], in the shielding cone. As a result, all [BPyPDI] signals are shifted upfield, and clearly, the magnitude of this effect depends on the distance between a given proton and the phthalocyanine core. Hence, the effect is particularly pronounced for the pyridyl substituents. Hereby, the H$^{3''}$ and H$^{5''}$ pyridyl protons display the strongest upfield shift appearing at δ = 2.14 ppm, followed by H$^{2''}$ and H$^{6''}$ with values of 5.28 ppm.

Insertion of the perylenediimide unit between the two [Ru(CO)Pc] rings completely eliminates any appreciable aggregation in solution. The signals corresponding, for example, to the [Ru(CO)Pc] appear sharp and well resolved for **1**, in contrast to those displayed by the phthalocyanine precursor (**2**). The lack of significant aggregation also allows the acquisition of ^{13}C NMR data for **1**; see Supporting Information. In this regard, the most significant feature is that of the carbonyl ligands coordinated to the Ru(II) ion at 179.5 ppm and the imido carbonyl at 161.1 and 160.8 ppm.

Electrochemical Studies. The first insight into donor−acceptor interactions came from electrochemical measurements, which were conducted to determine the donor and acceptor levels in [Ru(CO)Pc−BPyPDI−Ru(CO)Pc] **1** with (i) the individual components and (ii) the combined systems in *ortho*-dichlorobenzene and dichloromethane. For the electron-donating [Ru(CO)Pc] **2** the first reversible one-electron oxidation appears at +0.66 V, followed by a second reversible oxidation process at +1.42 V. Perylenediimide **3**, on the other hand, revealed the first reversible one-electron reduction around −0.6 V. In the combined system, namely, [Ru(CO)Pc−BPyPDI−Ru(CO)Pc] **1** the fingerprints that were seen for the individual components in terms of their oxidation and reduction processes were also registered. A closer inspection reveals, however, that the

(26) For some examples, see: (a) Cammidge, A. N.; Berber, G.; Chambrier, I.; Hough, P. W.; Cook, M. J. *Tetrahedron* **2005**, *61*, 4067−4074. (b) Berber, G.; Cammidge, A. N.; Chambrier, I.; Cook, M. J.; Hough, P. W. *Tetrahedron Lett.* **2003**, *44*, 5527−5529. (c) Hanack, M.; Osio-Barcina, J.; Witke, E.; Pohmer, J. *Synthesis* **1992**, 211−214. (d) Yanagisawa, M.; Korodi, F.; He, J.; Sun, L.; Sundström, V.; Akermark, B. *J. Porphyrins Phthalocyanines* **2002**, *6*, 217−224. (e) Rihter, B. D.; Kenney, M. E.; Ford, W. E.; Rodgers, M. A. J. *J. Am. Chem. Soc.* **1990**, *112*, 8064−8070.

(27) (a) Mak, C. C.; Bampos, N.; Darling, S. L.; Montalti, M.; Prodi, L.; Sanders, J. K. M. *J. Org. Chem.* **2001**, *66*, 4476−4486. (b) Webb, S. J.; Sanders, J. K. M. *Inorg. Chem.* **2000**, *39*, 5912. (c) Webb, S. J.; Sanders, J. K. M. *Inorg. Chem.* **2000**, *39*, 5912−5919.

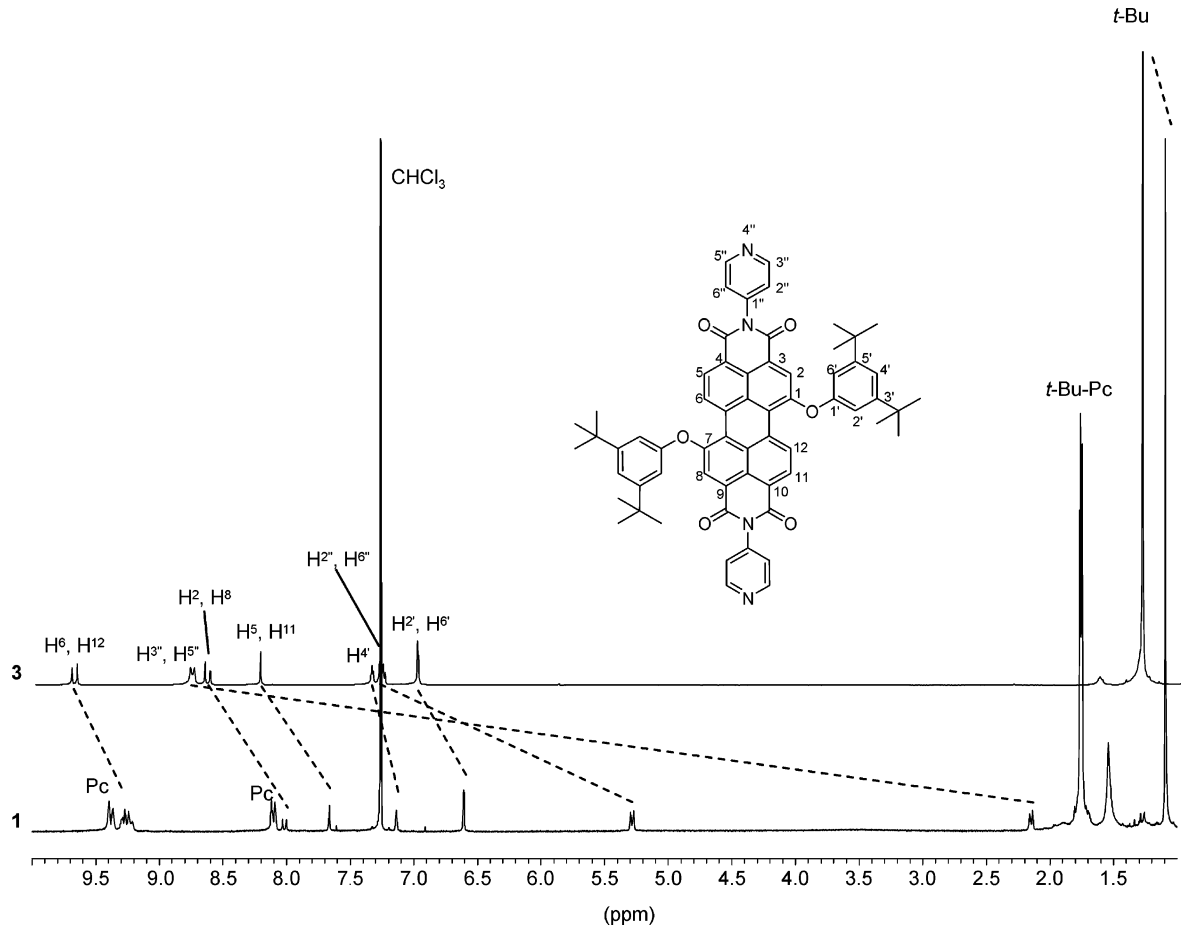

Figure 3. Comparison between ^{1}H NMR spectra in $CDCl_3$ for [BPyPDI] derivative **3** and cofacially assembled [Ru(CO)Pc−BPyPDI−Ru(CO)Pc] **1**.

oxidation peak is shifted to +0.74 V, while the reduction gives rise to a difference of 0.04 V.

Photophysical Studies - Fluorescence. Next, we probed the excited-state interactions by means of fluorescence spectroscopy. In the individual building blocks [BPyPDI] **3** emits quite strongly from the first singlet excited state (2.11 eV), with a maximum at 587 nm and a quantum yield of 0.75, while much weaker fluorescence is seen for [Ru(CO)Pc] **2** (1.87 eV), with a maximum at 660 nm and a quantum yield of 1.5×10^{-4} (Figure 4).[28] Both fluorescence patterns mirror image well the singlet ground-state spectra with minute Stokes shifts of 440 cm^{-1} ([BPyPDI] **3**) and 180 cm^{-1} ([Ru(CO)Pc] **2**). Time-resolved fluorescence experiments helped to shed light onto the different fluorescence quantum yields. In particular, we failed to see any appreciable fluorescence for [Ru(CO)Pc] **2** that exceeds the 100 ps resolution limit of our fluorescence apparatus. Therefore, we must assume, similar to the photophysics of the analogous tetraphenylporphyrin complex [Ru(TPP)(CO)(Py)], a nearly instantaneous singlet excited-state deactivation affording the long-lived triplet manifold.[22a] But in contrast to [Ru(TPP)(CO)(Py)] no triplet centered emission is seen for [Ru(CO)Pc] **2** in the 650−850 nm range. Basically, the ruthenium metal imposes a heavy atom effect, accelerating the spin-forbidden interconversion between the photoexcited singlet and triplet manifolds. Quite different in [BPyPDI] **3**, we see a long-lived fluorescence (6.4 ± 0.5 ns), which is in agreement with the high fluorescence quantum yields.

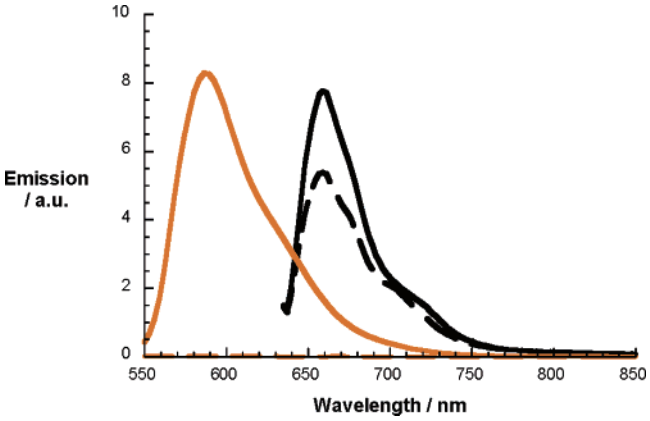

Figure 4. Steady-state room-temperature fluorescence spectra of [BPyPDI] **3** (orange solid spectrum) and [Ru(CO)Pc−BPyPDI−Ru(CO)Pc] **1** (orange dashed spectrum) in dichloromethane with matching absorption at the 530 nm wavelength (i.e., $OD_{530nm} = 0.2$) and [Ru(CO)Pc] **2** (black solid spectrum) and [Ru(CO)Pc−BPyPDI−Ru(CO)Pc] **1** (black dashed spectrum) in dichloromethane with matching absorption at the 630 nm excitation wavelength (i.e., $OD_{630nm} = 0.2$).

When inspecting [Ru(CO)Pc−BPyPDI−Ru(CO)Pc] **1**, we see relative to the aforementioned references significantly lower fluorescence quantum yields, regardless of exciting into the perylenediimide or into the phthalocyanine centered transitions at 560 or 655 nm, respectively. Important is the fact that the quenched fluorescence spectra retain the key pattern established

(28) The remarkable difference in fluorescence quenching relates to the different fluorescence lifetimes that [BPyPDI] **3** and [Ru(CO)Pc] **2** exhibit.

for the individual components and, therefore, their individual electronic identity. Notably, the extent of fluorescence quenching is much stronger for the [BPyPDI] moiety than for the [Ru(CO)Pc] unit with quantum yields of 0.001 and 1.1×10^{-4}, respectively (vide infra). In other words, quenching factors of 750 and 1.4 are determined for photoexcited [BPyPDI] and [Ru(CO)Pc], respectively. Importantly, when exciting at 560 nm (i.e., perylenediimide) no [Ru(CO)Pc] centered fluorescence was detected around 680 nm. This finding is helpful in ruling out a transduction of singlet excited-state energies from photoexcited [BPyPDI] to [Ru(CO)Pc], which is in a thermodynamic sense feasible with a driving force of 0.24 eV (vide infra).[29] In the next step, we employed the [BPyPDI] fluorescence (i.e., fluorescence quantum yields in **1** and **3** and fluorescence lifetime in **3**) to extrapolate the intramolecular deactivation as 1.1×10^{11} s^{-1}. Such an ultrafast deactivation points to an extremely efficient interplay between the [BPyPDI] and the [Ru(CO)Pc] moieties and resembles the deactivation seen in previous work on a [BPyPDI] derivative coordinated to a ruthenium tetraphenylporphyrin [Ru(TPP)(CO)(EtOH)].[22a]

Thermodynamic evaluations of the reaction pathways assist in evaluating the photoreactivity in [Ru(CO)Pc−BPyPDI−Ru(CO)Pc] **1**. The fluorescence maxima are used to estimate the singlet excited-state energy of [Ru(CO)Pc] and [BPyPDI] as 1.87 and 2.11 eV, respectively. The energy of the radical ion pairs were, as the sum of the oxidation and reduction potentials that is corrected by coulomb attractions,[30] 1.23 eV for [Ru(CO)Pc−BPyPDI−Ru(CO)Pc] **1** in dichloromethane and *ortho*-dichlorobenzene. Thus, our consideration supports exothermic charge separation scenarios that commence with the photoexcited [Ru(CO)Pc] ($-\Delta G_{ET} = -0.64$ eV) and [BPyPDI] ($-\Delta G_{ET} = -0.88$ eV). Consequently, charge separation and charge recombination reactions are likely to be located in the normal region or close to the thermodynamic maximum and deep in the inverted region of the Marcus parabola, respectively. In fact, we have calculated a solvent reorganization energy of 0.61 eV by employing a donor−acceptor separation of 12.3 Å and radii of 6.6 and 6.8 Å, while the internal reorganization has to be assumed with at least 0.3 eV.[31] Alternatively, a transduction of singlet excited-state energy, but only from [BPyPDI] to [Ru(CO)Pc] and not vice a versa, is thermodynamically quite plausible with an energy gap of 0.24 eV.

Photophysical Studies - Transient Absorption. Next, transient absorption spectroscopy (i.e., 150 fs laser pulses at 530 or 650 nm and 8 ns laser pulses at 355 or 532 nm) was employed to confirm the ultrafast singlet excited-state deactivations and, in addition, to characterize the nature of the photoproducts.

When photoexciting [BPyPDI] **3**, population of the singlet excited state leads to differential absorption changes that include a broad transient bleach between 450 and 655 nm and that is centered at 560 nm. In the red we see a transient maximum at 700 nm (i.e., singlet−singlet transition). The perylenediimide

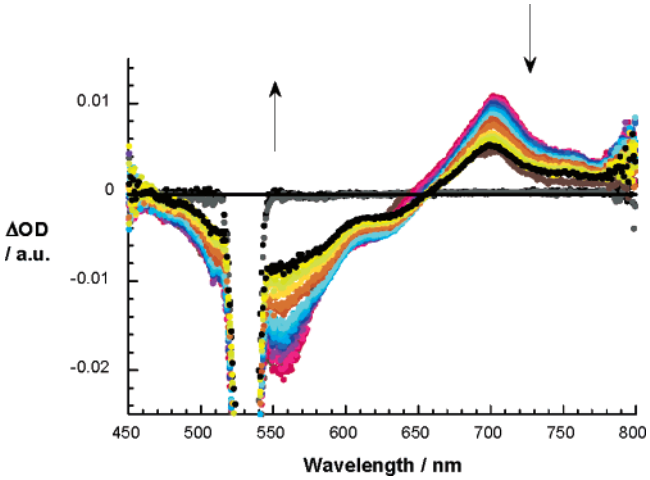

Figure 5. Differential absorption spectra (visible) obtained upon femtosecond flash photolysis (530 nm) of [BPyPDI] **3** in dichloromethane with several time delays between 0 and 1500 ps at room temperature; arrows indicating the singlet excited-state decay.

singlet excited features convert, as indicated in Figure 5 and supported by previous investigations, via an inefficient intersystem crossing (i.e., with low quantum yields) to the energetically lower lying triplet excited features.[22a,32] From the intersystem crossing, we approximate a singlet lifetime of 6.0 ± 0.5 ns (1.6×10^8 s^{-1}). Similarly, the metastable and fast decaying singlet−singlet features of [Ru(CO)Pc] **2** (i.e., maximum at 555 nm; minima at 585 and 650 nm; see Figure S12) also give rise to an intersystem crossing process that is, however, due to the presence of the ruthenium center, markedly accelerated. Important here is the very short singlet lifetime of 60 ± 0.2 ps (1.6×10^{10} s^{-1}). This value is in accordance with our fluorescence lifetime measurements, where no resolvable fluorescence decay was noted with our instrumental setup (i.e., instrument response time of around 100 ps). In the complementary recorded nanosecond spectra (see Figure 6) we see only the long-lived triplet−triplet transitions for the [Ru(CO)Pc] **2** and [BPyPDI] **3** building blocks. Under anaerobic conditions the triplet lifetimes are 12 μs for [Ru(CO)Pc] and 80 ns for [BPyPDI]. Both triplet excited states turned out to be quite oxygen sensitive and are quenched with nearly diffusion-controlled kinetics to afford the formation of singlet oxygen.

[Ru(CO)Pc−BPyPDI−Ru(CO)Pc] **1** shows initially after femtosecond laser excitation at either 530 nm (i.e., [BPyPDI]) or 650 nm (i.e., [Ru(CO)Pc]) differential absorption characteristics that resemble those seen in the reference systems, that is, the singlet−singlet attributes of either [Ru(CO)Pc] (i.e., maximum at 555 nm; minima at 585 and 650 nm; Figure 7) or [BPyPDI] (i.e., maximum at 700 nm; transient bleach between 450 and 655 nm; Figure 8).

Such observations are vital, since they affirm the successful photoexcitation of the two chromophores, despite the presence of the electron-donor or electron-acceptor moieties and their

(29) Despite the large driving force for charge separation, especially evolving from photoexcited [BPyPDI], no additional emission that might be attributable to a charge transfer is seen in the recorded range of up to 900 nm.

(30) Hauke, F.; Hirsch, A.; Liu, S.-G.; Echegoyen, L.; Swartz, A.; Luo, C.; Guldi, D. M. *Chem. Phys. Chem.* **2002**, *3*, 195−205.

(31) (a) Guldi, D. M.; Imahori, H.; Tamaki, K.; Kashiwagi, Y.; Yamada, H.; Sakata, Y.; Fukuzumi S. *J. Phys. Chem. A* **2004**, *108*, 541−548. (b) Guldi, D. M.; Rahman, G. M. A.; Marczak, R.; Matsuo, Y.; Yamanaka, M.; Nakamura, E. *J. Am. Chem. Soc.* **2006**, *128*, 9420−9427.

(32) (a) Margineanu, A.; Hofkens, J.; Cotlet, M.; Habuchi, S.; Stefan, A.; Qu, J.; Kohl, C.; Mullen, K.; Vercammen, J.; Engelborghs, Y.; Gensch, T.; De Schryver, F. C. *J. Phys. Chem. B* **2004**, *108*, 12242−12251. (b) Hayes, R. T.; Wasielewski, M. R.; Gosztola, D. *J. Am. Chem. Soc.* **2000**, *122*, 5563−5567. (c) van der Boom, T.; Hayes, R. T.; Zhao, Y.; Bushard, P. J.; Weiss, E. A.; Wasielewski, M. R. *J. Am. Chem. Soc.* **2002**, *124*, 9582−9590. (d) Weiss, E. A.; Ahrens, M. J.; Sinks, L. E.; Gusev, A. V.; Ratner, M. A.; Wasielewski, M. R. *J. Am. Chem. Soc.* **2004**, *126*, 5577−5584. (e) Kaletas, B. K.; Dobrawa, R.; Sautter, A.; Würthner, F.; Zimine, M.; De Cola, L.; Williams, R. M. *J. Phys. Chem. A* **2004**, *108*, 1900−1909.

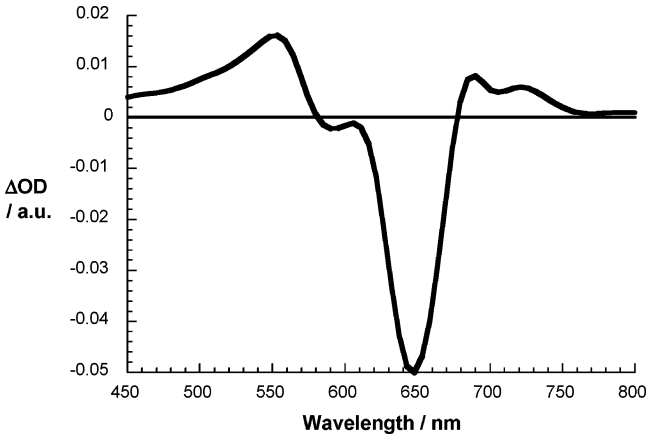

Figure 6. Differential absorption spectra (visible) obtained upon nanosecond flash photolysis (535 nm) of [Ru(CO)Pc] **2** in dichloromethane with a time delay of 50 ns at room temperature.

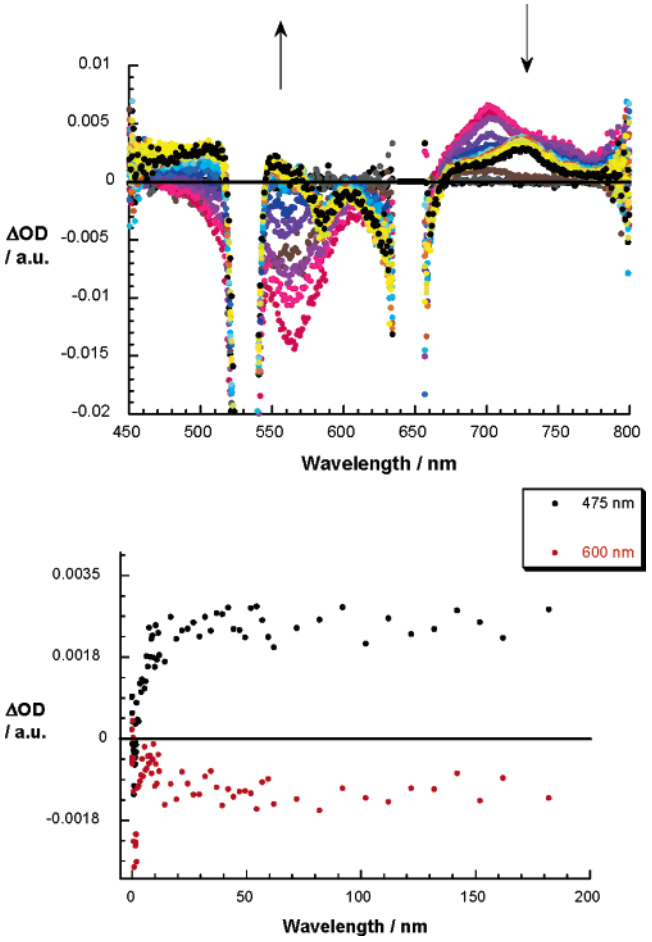

Figure 7. (Upper part) Differential absorption spectra (visible) obtained upon femtosecond flash photolysis (530 nm) of [Ru(CO)Pc−BPyPDI−Ru(CO)Pc] **1** in nitrogen saturated dichloromethane with several time delays between 0 and 1500 ps at room temperature. (Lower part) Time-absorption profiles of the spectra shown above at 475 and 600 nm, monitoring the formation of the [Ru(CO)Pc$^{\bullet+}$−BPyPDI$^{\bullet-}$− Ru(CO)Pc] radical ion pair state.

mutual electronic interactions. For [Ru(CO)Pc−BPyPDI−Ru(CO)Pc] **1** the singlet excited-state deactivations are, however, very fast; more precisely, singlet lifetimes of 19 ps (5.2×10^{10} s^{-1}) and 45 ps (2.2×10^{10} s^{-1}) were determined for the perylenediimide and phthalocyanine moieties, respectively. These values should be compared to the intersystem crossing

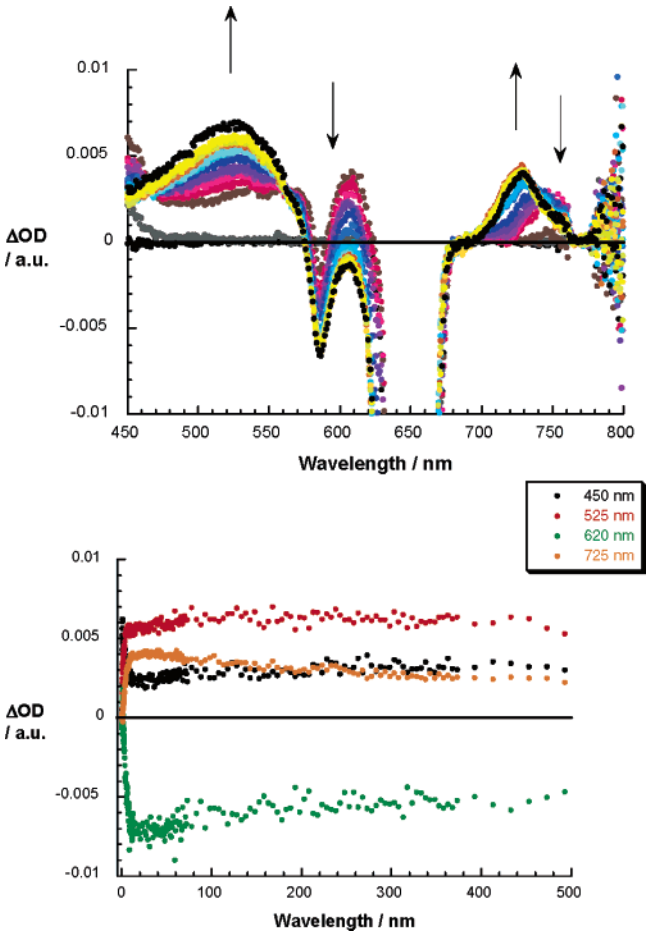

Figure 8. (Upper part) Differential absorption spectra (visible) obtained upon femtosecond flash photolysis (650 nm) of [Ru(CO)Pc−BPyPDI−Ru(CO)Pc] **1** in nitrogen saturated dichloromethane with several time delays between 0 and 1500 ps at room temperature. (Lower part) Time-absorption profiles of the spectra shown above at 450, 525, 620, and 725 nm, monitoring the formation of the [Ru(CO)Pc$^{\bullet+}$−BPyPDI$^{\bullet-}$−Ru(CO)Pc] radical ion pair state.

dynamics of 1.6×10^8 s^{-1} (i.e., [BPyPDI]) and 1.6×10^{10} s^{-1} (i.e., [Ru(CO)Pc]) yielding quenching factors of 325 and 1.4, respectively, and that resemble the fluorescence experiments. Deactivations evolve from the triplet excited states of either chromophore. Parallel with the decay of the singlet absorptions of either [Ru(CO)Pc] or [BPyPDI] units, new transient products are formed. While the products of these ultrafast decays bear no particular similarity with the triplet excited states, they are essentially identical for both pathways, that is, evolving from the [Ru(CO)Pc] singlet or the [BPyPDI] singlet. Features of the new product, as shown in Figures 7−9, are transient maxima at 530 and 725 nm, plus transient minima at 580 nm at 650 nm.

It is worth noting that when exciting the perylenediimide core in **1** at 530 nm, the product seems to bear no resemblance with those noted for the [Ru(CO)Pc] singlet excited-state features in **2** (Figures 6 and S12). Considering singlet lifetimes of 19 ps (i.e., [BPyPDI] in **1**) and 60 ps (i.e., [Ru(CO)Pc] in **2**), a potentially formed singlet [Ru(CO)Pc], as a product of singlet energy transfer, should, however, be detectable. Similarly, time-absorption profiles that represent the transformation of the [BPyPDI] singlet excited state to the final photoproduct reveal only a single component. Taken all the aforementioned facts into concert, we must infer that energy transfer between the

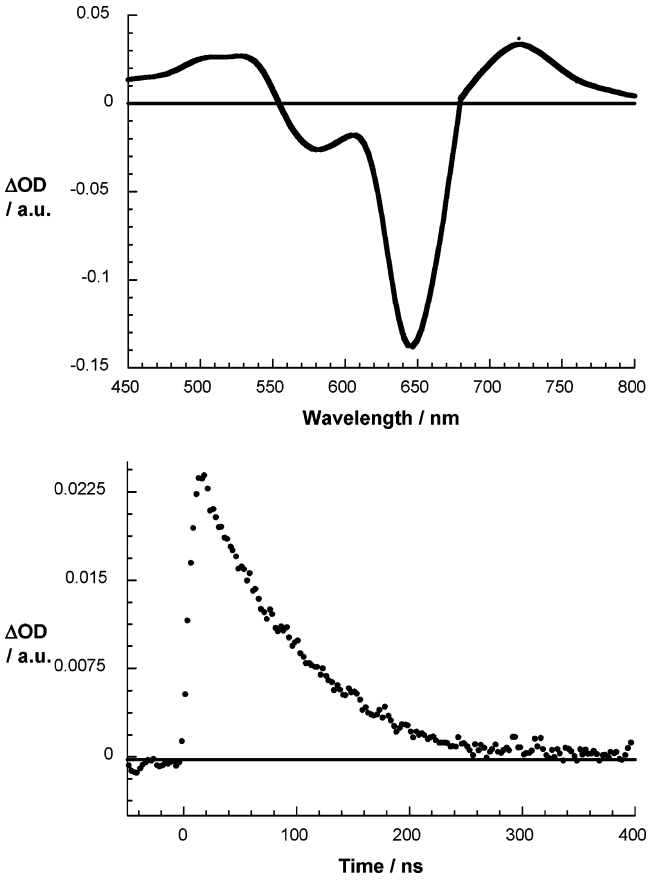

Figure 9. (Upper part) Differential absorption spectra (visible) obtained upon nanosecond flash photolysis (532 nm) [Ru(CO)Pc−BPyPDI−Ru(CO)Pc] **1** in nitrogen saturated dichloromethane with a time delay of 15 ns, showing the [Ru(CO)Pc$^{\bullet+}$−BPyPDI$^{\bullet-}$−Ru(CO)Pc] radical ion pair features. (Lower part) Time-absorption profiles of the spectrum shown above at 725 nm, monitoring the decay of the [Ru(CO)Pc$^{\bullet+}$−BPyPDI$^{\bullet-}$−Ru(CO)Pc] radical ion pair state.

two constituents (i.e., perylenediimide and phthalocyanine) plays no major rule.

To attribute our spectral observation pulse radiolysis experiments, reduction of perylenediimide **3** and oxidation of phthalocyanine **2**, were deemed necessary. Pulse radiolytic reduction was performed in a solvent mixture containing toluene, 2-propanol, and acetone, where in the absence of molecular oxygen strongly reducing $(CH_3)_2{}^{\bullet}COH$ and $(CH_3)_2{}^{\bullet}CO^-$ radicals are formed that are sufficiently reactive to reduce electron acceptors such as C_{60} and a number of fullerene derivatives.[33] The differential absorption spectrum following the conclusion of the radiolytic reduction of [BPyPDI] **3** is shown in Figure S13. Sets of maxima, at 725 nm, and minima, at 550 nm, are clearly discernible that are formed under pseudo first-order conditions. On the other hand, as solvent for the pulse radiolytic oxidation experiments of [Ru(CO)Pc] **2**, dichloromethane was chosen.[34] Under aerated conditions, that is, solvent ionization and subsequent reaction with molecular oxygen oxidative, peroxyl radicals are formed. Figure S13 gathers typical differential absorption changes that were recorded at the conclusion of the $^{\bullet}OOCH_2Cl$ or $^{\bullet}OOCHCl_2$ induced oxidation of [Ru(CO)Pc] **2** with a minimum at 650 nm and maxima at 530 and 725 nm.

When superimposing the features of the radiolytically generated [BPyPDI]$^{\bullet-}$ and [Ru(CO)Pc]$^{\bullet+}$, a remarkable agreement is achieved with the features seen in the 300 and 900 nm range of photoexcited [Ru(CO)Pc−BPyPDI−Ru(CO)Pc] **1** on the femto-, pico-, and nanosecond time scales. Thus, we ascribe the photolytically generated transitions to the composite spectrum of the one-electron reduced radical anion of [BPyPDI] and the one-electron oxidized radical cation of [Ru(CO)Pc].

On the femto- and picosecond time scale no significant decays of the radical ion pair state are noted. It is only in the complementary nanosecond transient absorption measurements (Figure 9) that the radical ion pair starts to undergo an intrinsically slow charge recombination. The product of this thermodynamically driven process, which is independent of photoexciting the [BPyPDI] or the [Ru(CO)Pc] moiety at 355 or 532 nm, respectively, is the quantitative reconstitution of the singlet ground state. The radical ion pair lifetime, which is on the order of 115 ± 5 ns, reveals a significant stabilization and confirms our earlier thermodynamic postulate, namely, that the strongly exothermic charge recombination dynamics are placed into the inverted region of the Marcus parabola. Additionally, placing donor and acceptor into an orthogonal geometry is expected to diminish the electronic coupling element and, consequently, to slow the charge recombination.

Notably, although the [BPyPDI] triplet excited state (i.e., 1.2 eV)[22a] is energetically lower placed than the corresponding radical ion pair state (1.23 eV), our spectroscopic analysis suggests that charge recombination leads to a recovery of the singlet ground state.[35] Figure 10 summarizes the energy level diagram of [Ru(CO)Pc−BPyPDI−Ru(CO)Pc] **1**.[36] This reactivity resembles that seen in similar electron-donor−acceptor hybrids and conjugates reported by Würthner and co-workers,[22a,32e] while it contrasts the findings seen by Fukuzumi et al.,[20c] who has detected the formation of a transient triplet excited state in the charge recombination process. Two rationales should be taken into consideration: (i) smaller energy gaps and (ii) the unique orthogonal geometry of [Ru(CO)Pc−BPyPDI−Ru(CO)Pc] **1** might favor the direct recovery of the ground state.

Conclusions

In summary, through simple coordination chemistry, a novel electron donor−acceptor hybrid composed of a perylene-(bis)-imide [BPyPDI] and two ruthenium(II) phthalocyanines [Ru(CO)Pc] is obtained, en route to new and versatile donor−acceptor ensembles. The array shows remarkable stability in solution due to the robustness of the Ru(II)-pyridyl bonds. Photoexcitation of either chromophore is followed by a rapid intraensemble charge separation to generate a radical ion pair state that lives for hundreds of nanoseconds. This is, however, in contrast to previous reports on an electron donor−acceptor hybrid (i.e., a bispyridylperylenediimide pigment coordinated to two ruthenium(II) porphyrins)[22a] and on an electron-donor−acceptor conjugate (i.e., perylenediimide bearing pyrenes).[32e] Only the exclusive excitations of the perylenediimide lead to charge separation, while the deactivations of the porphyrin and

(33) (a) Guldi, D. M.; Hungerbühler, H.; Janata, E.; Asmus, K.-D. *J. Phys. Chem.* **1993**, *97*, 11258. (b) Guldi, D. M. *J. Phys. Chem. B* **2000**, *104*, 1483.
(34) Shank, N. E.; Dorfman, L. M. *J. Chem. Phys.* **1970**, *52*, 4441.
(35) Considering, however, that the [BPyPDI] triplet excited state lifetime is intrinsically shorter than that of the corresponding radical ion pair state, it might be populated but would be spectroscopically invisible to us.
(36) The [Ru(CO)Pc] triplet excited state is approximated as 1.14 eV, when considering the same singlet−triplet energy gap in ZnPc, but accounting for a [Ru(CO)Pc] singlet excited state (1.87 eV) that is 0.07 eV higher than that of ZnPc (see ref 11h).

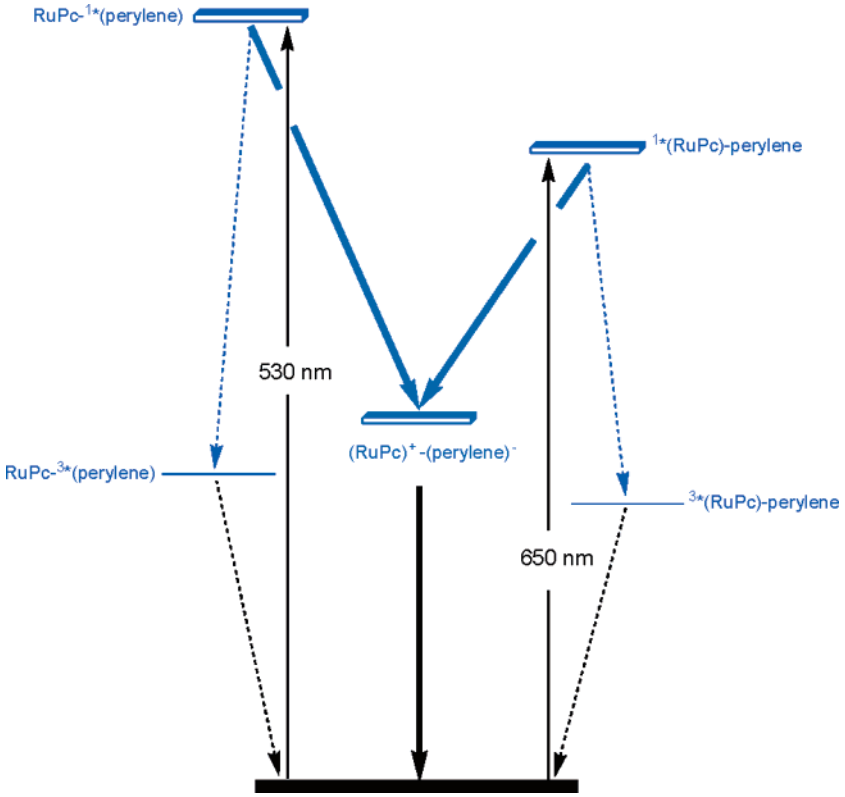

Figure 10. Energy level diagram of [Ru(CO)Pc−BPyPDI−Ru(CO)Pc] **1**.

pyrene are dominated by energy transfer. Notably, in donor−acceptor hybrids the radical ion pair lifetimes, depending on donor−acceptor separation, electronic coupling, etc., vary from as short as 27−39 ps to 1.6 s.[31,37] A more sensitive comparison involves similar bispyridylperylenediimide-based hybrids, where, however, only moderate lifetimes of up to 270 ps are registered.[22a] Owing to the efficiency of the synthetic method, in terms of both the good yield obtained and the high control of the geometry and stoichiometry of the assembly, as well as its versatility, a variety of metal-coordinated arrays with interesting photophysical features can be designed and prepared, and they are expected to be the object of future reports.

Experimental Section

General. Synthesis: UV/vis spectra were recorded with a Hewlett-Packard 8453 instrument. IR spectra were recorded with Bruker Vector 22 spectrophotometer. FAB-MS spectra were determined on a VG AutoSpec instrument. MALDI-TOF MS and HRMS spectra were recorded with a Bruker Reflex III spectrometer. NMR spectra were recorded with Bruker WM-200-SY and Bruker AC-300 instruments. Column chromatographies were carried out on silica gel Merck-60 (230−400 mesh, 60 Å), and TLC was performed on aluminum sheets precoated with silica gel 60 F_{254} (E. Merck). $Ru_3(CO)_{12}$ was purchased from Strem. Tetra-*tert*-butylphthalocyanine and all the other chemicals were purchased from Aldrich Chemical Co. and used as received without further purification.

Photophysics: Femtosecond transient absorption studies were performed with 530 and 650 nm laser pulses (1 kHz, 150 fs pulse width) from an amplified Ti:Sapphire laser system (model CPA 2101, Clark-MXR Inc.). Nanosecond laser flash photolysis experiments were performed with 355- or 532-nm laser pulses from a Quanta-Ray CDR Nd:YAG system (6 ns pulse width) in a front face excitation geometry. Fluorescence lifetimes were measured with a Laser Strope Fluorescence Lifetime spectrometer (Photon Technology International) with 337-nm laser pulses from a nitrogen laser fiber-coupled to a lens-based T-formal sample compartment equipped with a stroboscopic detector. Details of the Laser Strobe systems are described on the manufacture's web site. Emission spectra were recorded with an SLM 8100 spectrofluorometer. The experiments were performed at room temperature. Each spectrum represents an average of at least five individual scans, and appropriate corrections were applied whenever necessary.

Pulse Radiolysis: Pulse radiolysis experiments were performed using 50 ns pulses of 15 MeV electrons from a linear electron accelerator (LINAC). Dosimetry was based on the oxidation of SCN^- to $(SCN)_2^{\bullet-}$ which in aqueous, N_2O-saturated solution takes place with $G \approx 6$ (G denotes the number of species per 100 eV, or the approximate μM concentration per 10 J of absorbed energy). The radical concentration generated per pulse was varied $(1-3) \times 10^{-6}$ M.

Electrochemistry: Electrochemical measurements were performed at room temperature in a cell with three electrodes, containing 0.1 M tetrabutylammonium hexafluorphosphate ($TBAPF_6$) as the supporting electrolyte. A glassy carbon (2 mm ϕ) was used as the working electrode, and a platinum mesh and a silver wire were employed as the counter and the reference electrodes, respectively. Prior to each voltammetric measurement, the cell was degassed with Ar, the solvent was ODCB, and the sweep rate was 100 mV s^{-1}. The electrochemical measurements were performed using a concentration of 0.4 mM **3**, 0.3 mM **2**, and 0.2 mM **1**.

[Carbonyl-2(3),9(10),16(17),23(24)-tetrakis-*tert*-butylphthalocyaninato]Ru(II) (2). A mixture of tetra-*tert*-butylphthalocyanine (100 mg, 0.13 mmol), $Ru_3(CO)_{12}$ (173 mg, 0.27 mmol) and phenol (6 g) was heated at reflux temperature under argon for 8 h. The solution was allowed to cool to room temperature, and then it was dissolved in 50 mL of ethanol. After addition of water (200 mL) the resulting blue precipitate was filtered, washed with a 4:1 mixture of water and methanol, and dried. The crude was purified by column cromatography on silica gel using toluene and then chloroform as eluents. The solid

(37) Imahori, H.; Guldi, D. M.; Tamaki, K.; Yoshida, Y.; Luo, C.; Sakata, Y.; Fukuzumi, S. *J. Am. Chem. Soc.* **2001**, *123*, 6617−6628.

was suspended in hexanes, filtered, washed with the same solvent and dried at 90 °C and 10^{-1} mmHg, affording 96 mg (82%) of **2** as a deep blue solid; ^{1}H NMR (200 MHz, DMSO-d_6): δ = 9.4−9.0, (broad multiplet, 8H, H arom), 8.3−8.0, (broad multiplet, 4H, H arom), 1.72, 1.62, 1.59, (3 s, 36H, C(CH$_3$)$_3$); IR (KBr): ν = 2951, 2910, 2870 (C−H), 2042, 1958 (C═O), 1649, 1609, 1485, 1450, 1391, 1323, 1256, 1192, 1124, 1043, 935, 827, 766, 679 cm^{-1}; UV/vis (CHCl$_3$): λ_{max} (log ϵ) = 296 (5.01), 330 (4.56), 345 (4.53), 552 (3.50), 569 (3.80), 590 (4.42), 627 (sh), 652 nm (5.18); MS (MALDI-TOF, TCNQ): m/z = 863−869 [M + H]$^+$, 835−841 [M − CO + H]$^+$; HRMS (MALDI-TOF): calcd for $C_{49}H_{48}N_8O^{96}Ru$, 860.303; found, 860.306. Anal. Calcd for $C_{49}H_{48}N_8ORu\cdot 2H_2O$: C, 65.24; H, 5.81; N, 12.42. Found: C, 65.42; H, 5.85; N, 12.12.

***N,N′*-Di(4-pyridyl)-1,7-bis(3′,5′-di-*tert*-butylphenoxy)perylene-3,4:9,10-tetracarboxylic Acid Bisimide (3).** A solution of 1,7-bis(3′,5′-di-*tert*-butylphenoxy)perylene-3,4:9,10-tetracarboxydianhydrid[17c] (136 mg, 0.170 mmol), 4-aminopyridine (54 mg, 0.57 mmol) and Zn(OAc)$_2$ (17 mg, 0.09 mmol) in quinoline (6 mL) was refluxed under argon for 24 h. After cooling to room temperature the mixture was poured into 2 N HCl (28 mL). The resulting precipitate was filtered, washed with water and dried. The crude was chromatographed on silica gel using a 100:1 mixture of dichloromethane and methanol and then a 10:1 mixture of the same solvents. The second fraction was recrystallized from dichloromethane/hexanes and dried at 90 °C and 10^{-1} mmHg affording 121 mg (75%) of **3** as a dark red solid. ^{1}H NMR (200 MHz, CDCl$_3$): δ = 9.70 (d, J = 8.0 Hz, 2H, H^6, H^{12}), 8.77 (d, J = 6.5 Hz, 4H, H$^{3''}$, H$^{5''}$),8.65 (d, J = 8.0 Hz, 2H, H^2, H^8), 8.23 (s, 2H, H,^{5} H^{11}), 7.36 (d, J = 1.5 Hz, 2H, H$^{4'}$), 7.28 (d, J = 6.5 Hz, 4H, H$^{2''}$, H$^{6''}$), 7.00 (d, J = 1.5 Hz, 4H, H$^{2'}$, H$^{6'}$),1.31 (s, 36H, C(CH$_3$)$_3$); ^{13}C NMR (75.5 MHz, CDCl$_3$): δ = [162.6, 162.2] (N−C═O), 156.4, 154.0, 151.0, 142.7, 133.9, 130.7, 130.3, 129.3, 129.2, 124.7, 123.9, 123.2, 123.1, 122.9, 121.6, 121.0, 120.1, 119.5, 114.6, 35.1 (*C*(CH$_3$)$_3$), 31.3 (C(*C*H$_3$)$_3$); IR (KBr): ν = 2957, 2905, 2870 (C−H), 1709, 1668 (N−C═O), 1589, 1499, 1408, 1342, 1261, 1194, 1070, 941 cm^{-1}; UV/vis (CHCl$_3$): λ_{max} (log ϵ) = 245 (4.73), 269 (4.63), 408 (3.91), 484 (sh), 519 (4.41), 557 nm (4.59); MS (MALDI-TOF, Dithranol): m/z = 953 [M + H]$^+$; HRMS (MALDI-TOF): calcd for $C_{62}H_{57}N_4O_6$, 953.426; found, 953.426. Anal. Calcd for $C_{62}H_{56}N_4O_6$: C, 78.13; H, 5.92; N, 5.88. Found: C, 78.50; H, 6.04; N, 6.13.

[Ru(CO)Pc−BPyPDI−Ru(CO)Pc] (1). A solution of **2** (25 mg, 0.025 mmol) and **3** (10 mg, 0.01 mmol) in chloroform (4 mL) was stirred under argon at room temperature and protected from light for 12 h. The solvent was rotary evaporated, and the residue was suspended in hexanes, filtered, and washed with hexanes and then with methanol. The solid was recrystallized from dichloromethane/hexane and dried at 90 °C and 10^{-1} mmHg yielding 20 mg (68%) of **1** as a violet-blue solid; ^{1}H NMR (200 MHz, CDCl$_3$): δ = 9.37 (d, J = 8.0 Hz, 8H, H^{Pc}), 9.3−9.2 (m, 10H, H^{Pc}, H,^{6} H^{12}), 8.11 (d, J = 8.0 Hz, 8H, H^{Pc}), 8.01 (d, J = 8.0 Hz, 2H, H^2, H^8), 7.66 (s, 2H, H,^{5} H^{11}), 7.13 (d, J = 1.5 Hz, 2H, H$^{4'}$), 6.60 (d, J = 1.5 Hz, 4H, H$^{2'}$, H$^{6'}$), 5.28 (d, J = 7.0 Hz, 4H, H$^{2''}$, H$^{6''}$), 2.14 (d, J = 7.0 Hz, 4H, H$^{3''}$, H$^{5''}$), 1.76, 1.75, 1.75, 1.74 (4s, 72H, C(CH$_3$)$_3^{Pc}$), 1.09 (s, 36H, C(CH$_3$)$_3$); ^{13}C NMR (75.5 MHz, CDCl$_3$): δ = 179.49 (C═O) [161.14, 160.78] (N−C═O), 153.69, 153.54, 152.50, 145.27, 144.36, 144.34, 144.30, 144.29, 144.25, 144.22, 144.19, 144.14, 144.11, 144.09, 144.06, 141.72, 139.78, 139.69, 137.35, 137.31, 130.11, 128.71, 128.67, 128.66, 126.44, 126.41, 126.35, 123.02, 122.53, 122.51, 122.05, 121.76, 120.66, 120.56, 119.68, 118.62, 114.10, [35.79, 35.75, 34.90] (*C*(CH$_3$)$_3$), [32.02, 31.99, 31.13] (C(*C*H$_3$)$_3$); IR (KBr): ν = 2955, 2908, 2862 (C−H), 1969 (C═O), 1713, 1678 (N−C═O), 1632, 1597, 1481, 1400, 1331, 1261, 1192, 1122, 1053, 937, 822, 752 cm^{-1}; UV/vis (CHCl$_3$): λ_{max} (log ϵ) = 247 (4.97), 300 (5.19), 329 (4.83), 347 (4.78), 410 (3.89), 486 (sh), 523 (4.40), 565 (4.68), 588 (4.76), 651 nm (5.43); MS (MALDI-TOF, TCNQ): m/z = 2679−2692 [M + H]$^+$, 2273−2285 [M − [(*t*-Bu)$_2$C$_6$H$_3$O]]$^+$, 953, 863−869, 835−841. Anal. Calcd for $C_{160}H_{152}N_{20}O_8Ru_2\cdot 2H_2O$: C, 70.62; H, 5.78; N, 10.29. Found: C, 70.79; H, 5.94; N, 10.11.

Acknowledgment. Funding from EU (STREP − FP6-2003-NMP-TI-3-Main), MEC (Spain − CTQ2005-08933/BQU) Comunidad de Madrid (Spain − S-0505/PPQ/000225), Deutsche Forschungsgemeinschaft (SFB 583), FCI, and Office of Basic Energy Sciences of the U.S. Department of Energy (NDRL-4696) are gratefully acknowledged. M.S.R.-M also acknowledges MEC (Spain) for a Ramón y Cajal research position.

Supporting Information Available: Complete ref 2c, characterization data for new compounds **1**−**3** (^{1}H NMR, ^{13}C NMR, IR, MS, femtosecond transient absorption, radiolytic transient absorption spectra). This material is available free of charge via the Internet at http://pubs.acs.org.

JA0622195